Ion-electron correlations in liquid metals from orbital-free *ab initio* molecular dynamics

J. A. Anta, B. J. Jesson, and P. A. Madden
Physical and Theoretical Chemistry Laboratory, Oxford University, South Parks Road, Oxford OX1 3QZ, United Kingdom
(Received 23 December 1997)

Extensive *ab initio* molecular-dynamics (AIMD) simulations have been performed for liquid Na, Mg, and Al, three metals having the same core of 10 electrons but with a different number of valence electrons. The calculations have been carried out with the orbital-free version of the Car-Parrinello technique. Results were obtained for the functions that describe the ion-ion and ion-electron correlations. Comparison of these with results of those from standard Kohn-Sham AIMD confirms the ability of the orbital-free scheme to provide correct properties from first principles at a reasonable computational cost. The results presented here demonstrate that the overall ion-electron correlations predicted by simulation differ substantially from the experimental data so far reported for this property. This observation is closely related to the fact that, according to the theory, the difference between x-ray and neutron-diffraction structure factors should be much smaller than that encountered in the experiments. [S0163-1829(98)04834-6]

I. INTRODUCTION

A liquid metal can be regarded as a mixture of positively charged ions and nearly-free electrons, an intuitive picture that has been extensively exploited in many theoretical works.[1–7] As first pointed out by Egelstaff, March, and McGill,[2] the existence of electrons that are not attached to the ions leads to the structure factors measured by neutron-, x-ray-, and electron-diffraction experiments being slightly different from each other. From this analysis, it is concluded that it should be possible, in principle, to extract the ion-electron partial structure factor from the comparison of various types of diffraction data. A more rigorous treatment than that of Egelstaff, which involved just neutron and x-ray diffraction, has been discussed by Chihara.[4] His work has been followed by several efforts to assess the magnitude and shape of the ion-electron correlation from experimental measurements.[8–10]

The first theoretical attempts to determine the ion-electron correlation were undertaken in the framework of linear-response theory (LRT).[5,11] The ion-electron partial structure factor can be related to the ion-ion structure factor via the screening density function that is in turn related to the dielectric or linear-response function. The case of Na (and other alkalis[11]) is particularly well studied. Linear-response-based predictions for this system give results that depend on the assumed form of the pseudopotential.[5,11] Ion-ion and ion-electron correlations in Na (Ref. 6) and Al (Ref. 7) have also been studied by means of the Quantal hypernetted chain equation. In this case theory and experiment evince clear disagreement, even for the ion-ion structure factor.

Ab initio molecular-dynamics methods,[12,13] based on density-functional theory (DFT),[14] provide a direct method to calculate ion-ion, ion-electron, and electron-electron correlations since they contain an explicit representation of the valence electron density. A first attempt of this type was made by de Wijs *et al.*,[15] who performed Kohn-Sham Car-Parrinello molecular-dynamics (KS-AIMD) simulations for liquid Mg and Bi. They reported results for the ion-ion and ion-electron microscopic structure of these metals. Their comparison with experiment, although excellent with regard to the ion-ion structure factor and pair-correlation function, brought out a striking discrepancy for the functions that describe the ion-electron correlation. Due to the pseudopotential approximation, the electronic structural data provided by the AIMD simulations are not accurate at distances close to the atomic nuclei. Nevertheless, as already stressed by de Wijs *et al.*,[15] this does not affect the region in which the discrepancy between experiment and simulation for the ion-electron correlation is most pronounced.

An alternative to the KS formulation of the Car-Parrinello method, the so-called orbital-free (OF) *ab initio* molecular-dynamics (OF-AIMD),[16–19] offers an attractive approach to the problem. By dispensing with the orbitals of the Kohn-Sham formulation, the OF-AIMD method takes full advantage of the Hohenberg-Kohn theorem and provides a simulation method that scales almost linearly with system size.[18] It therefore becomes possible to perform simulations with larger numbers of particles and to carry out longer runs than for KS-AIMD, thereby achieving greater statistical precision. The OF-AIMD method has already been used to obtain the ion-ion structure factor of liquid sodium.[18] It has also been shown to describe correctly static and dynamic properties of solid Na (Ref. 16) and Al.[19] Recently, Watson *et al.*[20] have devised a method for producing *ab initio* local pseudopotentials for application in OF-AIMD. The basic idea is to construct pseudopotentials that render, when introduced within the OF scheme, the same results for the electron density as those of KS calculations with *ab initionon-local* pseudopotentials in an appropriate reference state. This method, together with the OF-AIMD simulation itself, affords a fully first-principles procedure suitable for studying metallic systems. We will discuss this point thoroughly when analyzing our results.

In this paper we have used the OF-AIMD method and the pseudopotential generation scheme to simulate liquid Na, Mg, and Al near their melting points. Following Takeda *et al.*,[10] we have chosen these metals since they possess the same core of 10 electrons, but have one, two, and three valence electrons, respectively. This should lead to a system-

atic variation in the ion-electron correlations as we move from Na to Al. The purpose of our calculations is twofold. On the one hand, we attempt to test the ability of the simulation method itself to provide correct structural data in the liquid state as an alternative to the computationally more expensive KS-AIMD scheme. In this regard, the most significant comparison is with the results of de Wijs *et al.* for Mg. However, we are also interested in the comparison with the ion-electron structure factor predicted by linear-response theory, to which our results would be expected to agree exactly if the pseudopotentials in these metals were sufficiently weak. We will show that the calculated ion-electron structure factor evolves in a readily interpretable way from Na to Al. On the other hand, we will compare the results yielded by the simulations with the available experimental data in order to clarify the actual significance of the ion-electron structure factors derived so far from scattering measurements. In this regard, the route that we have used is complementary to the experimental one. Starting from the calculated partial structure factors, we have evaluated a theoretical estimate of the difference between the x-ray- and neutron-diffraction structure factors, which may be directly compared with the experimentally obtained difference from which the ion-electron correlations are extracted. By these means, we expose the importance of the treatment of the incoherent x-ray scattering by the valence electrons and the requirements on the experimental resolution in the two experiments in order to extract the desired quantity.

II. THEORETICAL BACKGROUND

A. The Ashcroft-Langreth partial structure factors

As mentioned in the Introduction, a metal can be treated as a mixture of ions and electrons. Under this assumption, a convenient method of describing all correlations occurring in the system is in terms of Ashcroft-Langreth (AL) partial structure factors[1]

$$S_{ij}(\mathbf{k}) = \delta_{ij} + \sqrt{N_i N_j} \int [g_{ij}(\mathbf{r}) - 1] e^{i\mathbf{k}\cdot\mathbf{r}} d\mathbf{r}, \tag{1}$$

where N_i and N_j are, respectively, the number of particles of species i and j, and g_{ij} is the pair distribution function. This expression can be shown to be equivalent to[21]

$$S_{ij}(\mathbf{k}) = \frac{1}{\sqrt{N_i N_j}} \langle \rho_i(\mathbf{k}) \rho_j(-\mathbf{k}) \rangle, \tag{2}$$

where $\rho_i(\mathbf{k})$ is the $\mathbf{k}$th Fourier component of the number density of species i and $\langle \cdots \rangle$ denotes averaging over the positions of ions *and* electrons. If the system is homogeneous, both the structure factors and the pair distribution functions depend only on the modulus of $\mathbf{k}$ and $\mathbf{r}$, respectively. Equation (2) is computationally more convenient in the context of AIMD, as we will see below. Our task will then be to evaluate the three structure factors $S_{II}(k)$, $S_{Ie}(k)$, and $S_{ee}(k)$ (describing, respectively, ion-ion, ion-electron, and electron-electron correlations), as well as their corresponding distribution functions $g_{II}(r)$, $g_{Ie}(r)$, and $g_{ee}(r)$.

To simulate a real system, we use a small number of particles confined in a cubic cell that is periodically replicated in all directions. As a consequence of this, the electron density of the conduction electrons $\rho_e(\mathbf{r})$ is a periodic function and, therefore, can be expanded in a Fourier series

$$\rho_e(\mathbf{r}) = \sum_{\mathbf{k}} \rho_e(\mathbf{k}) e^{i\mathbf{k}\cdot\mathbf{r}} \tag{3}$$

with

$$\mathbf{k} = \frac{2\pi}{L}(m,n,l); \quad k^2 < K_{cut}^2, \tag{4}$$

where L is the side length of the simulation box, m,n,l are integers, and K_{cut} is the *spherical* cutoff in the plane-wave expansion. In addition, the following constraint is implemented:

$$\rho_e(0) = \frac{N_e}{V}, \tag{5}$$

where N_e is the total number of valence electrons and V is the volume of the system. In AIMD the Fourier coefficients of the number density of the ions $[\rho_I(\mathbf{k})]$ and of the valence electron density that minimizes the electronic energy functional at each ionic configuration (the ''adiabatic electron density'') are directly available and can be used in the calculation of these structure factors.

B. Neutron- and x-ray-diffraction structure factors

X-rays are scattered by electrons and the scattering amplitude is related to the number density of electrons $\rho(\mathbf{r})$ via[4]

$$I_X(\mathbf{k}) = \langle \rho(\mathbf{k}) \rho(-\mathbf{k}) \rangle, \tag{6}$$

where $\langle \cdots \rangle$ refers to a thermal (and quantal) average over the positions of ions *and* electrons. The x-ray-diffraction structure factor is conventionally defined as

$$S_X(k) = \frac{I_X^{coh}(k)}{N f_A^2(k)}, \tag{7}$$

$f_A(k)$ and N being the form factor of the isolated atom and the total number of atoms, respectively. Thus, $S_X(k)$ is obtained by eliminating the incoherent part from the experimental data. We now consider how, following Chihara,[4] this is achieved for a metal in a two-step procedure.

We first separate the contribution of the ionic cores. We write

$$\rho(\mathbf{k}) = f_I(\mathbf{k}) \rho_I(\mathbf{k}) + \rho_e(\mathbf{k}), \tag{8}$$

where $\rho_e(\mathbf{k})$ is the valence electron density and $f_I(\mathbf{k})$ is the *ionic* form factor, i.e., the Fourier transform of the ground-state ionic electron density. However, we must recognize that in replacing the instantaneous core density by its average value, we are ignoring the incoherent scattering by the cores, due to Compton effects, and these must be reintroduced in the expression for the total scattering. Using Eq. (8), the total scattering function (6) can be split up into several terms involving partial AL structure factors and the incoherent core scattering[4]

$$I_X(k)/N = f_I^2(k)S_{II}(k) + 2\sqrt{z}f_I(k)S_{Ie}(k) + zS_{ee}(k) + (Z-z)S_{inc}^I(k); \quad k \neq 0. \tag{9}$$

Here Z is the atomic number, z is the number of valence electrons, and $S_{inc}^I(k)$ stands for the incoherent scattering of the *core* electrons.

We next separate the part of the valence density $\rho_e(k)$ that is correlated with the ion positions

$$\rho_e(\mathbf{k}) = \frac{\langle \rho_e(\mathbf{k})\rho_I(-\mathbf{k})\rangle}{\langle \rho_I(\mathbf{k})\rho_I(-\mathbf{k})\rangle}\rho_I(\mathbf{k}) + \delta\rho_e(\mathbf{k}) \equiv n(\mathbf{k})\rho_I(\mathbf{k}) + \delta\rho_e(\mathbf{k}). \tag{10}$$

The correlated part of the valence density is the adiabatic average electron density and $\delta\rho_e(\mathbf{k})$ is the part of the instantaneous valence electron density not correlated with the ion positions. We can rewrite Eq. (10) in real space as

$$\rho_e(\mathbf{r}) = \sum_{I=1}^{N} n(\mathbf{r}-\mathbf{R}_I) + \delta\rho_e(\mathbf{r}). \tag{11}$$

$n(\mathbf{r})$ is the so-called *screening density*,[5] which represents, on average, the fraction of valence electron density that surrounds each ion relative to the uniform background. If we introduce Eq. (10) in the definition of the partial structure factors involving the valence electron density, we arrive at

$$S_{Ie}(k) = \frac{1}{\sqrt{z}}n(k)S_{II}(k), \tag{12}$$

$$S_{ee}(k) = \frac{1}{z}n(k)S_{II}(k) + \langle \delta\rho_e(\mathbf{k})\,\delta\rho_e(-\mathbf{k})\rangle. \tag{13}$$

The last term in Eq. (13) corresponds to the structure factor of the uniform electron gas, since $\delta\rho_e(\mathbf{k})$ is explicitly independent of the ionic positions. According to Chihara,[4] this contribution leads (at $k \neq 0$) to incoherent scattering and, therefore, should be subtracted in the expressions above to estimate the correct x-ray-diffraction structure factor. Bearing this in mind, the *coherent* scattering function is

$$I_X^{coh}(k)/N = |f_I(k) + n(k)|^2 S_{II}(k), \tag{14}$$

where we have used Eqs. (12) and (13). The x-ray structure factor is then

$$S_X(k) = \frac{|f_I(k)+n(k)|^2}{|f_A(k)|^2}S_{II}(k). \tag{15}$$

In contrast to x-rays, neutrons are scattered by nuclei at the center of ions, and for that reason, the corresponding diffraction intensity is related to the number density of ions

$$I_N(\mathbf{k}) = b^2\left\langle \sum_{\alpha\beta} e^{-i\mathbf{k}\cdot(\mathbf{R}_\alpha - \mathbf{R}_\beta)}\right\rangle = b^2\langle \rho_I(\mathbf{k})\rho_I(-\mathbf{k})\rangle = Nb^2 S_{II}(\mathbf{k}), \tag{16}$$

where b is the scattering length of the nuclei. The neutron-diffraction structure factor is now defined as

$$S_N(k) = \frac{I_N(k)}{Nb^2} = S_{II}(k). \tag{17}$$

In conclusion, the availability of the partial structure factors S_{II}, S_{Ie}, and S_{ee}, from AIMD makes it possible to estimate, theoretically, the x-ray- and neutron-diffraction structure factors as well as their difference.

C. Orbital-free AIMD

In the OF-AIMD method,[16–19] the coefficients $\rho_e(\mathbf{k})$ occurring in Eq. (3) are taken to be virtual dynamic variables associated with ''fake'' masses μ_k. These coefficients evolve in time coupled with the ionic movement in accordance with the following equations of motion:[16,18]

$$\mu_k\ddot{\rho}_e(\mathbf{k}) = -\frac{\delta E(\rho_e;\{\mathbf{R}_I\})}{\delta\rho_e(\mathbf{k})}, \tag{18}$$

$$M\ddot{\mathbf{R}}_I = -\nabla_I E(\rho_e;\{\mathbf{R}_I\}) - \nabla_I V_{II}; \quad I = 1,2,\ldots,N. \tag{19}$$

In the expressions above, V_{II} is the potential energy of the ion-ion interaction, N is the total number of ions, and E is the electronic energy for a given configuration of ions $\{\mathbf{R}_I\}$. According to the basic theorem of DFT,[14] E is a functional of the electron density ρ_e. In the context of the OF formulation, such a functional is expressed without the introduction of orbitals,[16] in contrast to the more standard KS formulation that employs monoelectronic or bielectronic wave functions (orbitals) to represent the kinetic-energy functional. OF kinetic-energy functionals have been devised that reproduce the energetics of metals like Na and Al with the accuracy of KS calculations.[16,19] This treatment makes the electronic part of the computation formally of order $N \ln N$ and, because it is possible to ''precondition''[16] the AIMD fake dynamics, the whole dynamics scales linearly with the number of particles.

A crucial point in the evaluation of the electronic energy functional is the ion-electron interaction. Unless we perform a computationally very expensive all-electron calculation, this interaction must be described via a *pseudopotential* that is, in principle, *nonlocal*.[1,22] Unfortunately, the OF method does not allow for the use of nonlocal pseudopotentials as it is based purely on the electron density. As already mentioned in the Introduction, this drawback can be surmounted by means of the method recently proposed by Watson *et al.*[20] By using their procedure, it is possible to obtain local pseudopotentials from first principles that can be readily utilized in OF-AIMD simulations. The methodology adopted to generate a local pseudopotential suitable for OF-AIMD simulations consists basically of three stages: (1) all-electron KS calculation in a single atom and subsequent *pseudisation* to obtain an initial *nonlocal* pseudopotential, (2) extensive KS calculations in the solid[23] phase using this nonlocal pseudopotential, (3) inversion of the solid-phase KS electron density by means of the OF functional in order to extract the *local* pseudopotential to be used in the molecular-dynamics calculations.

In AIMD, we simulate only the *adiabatic* valence electron density, so, comparing with the discussion of the experimen-

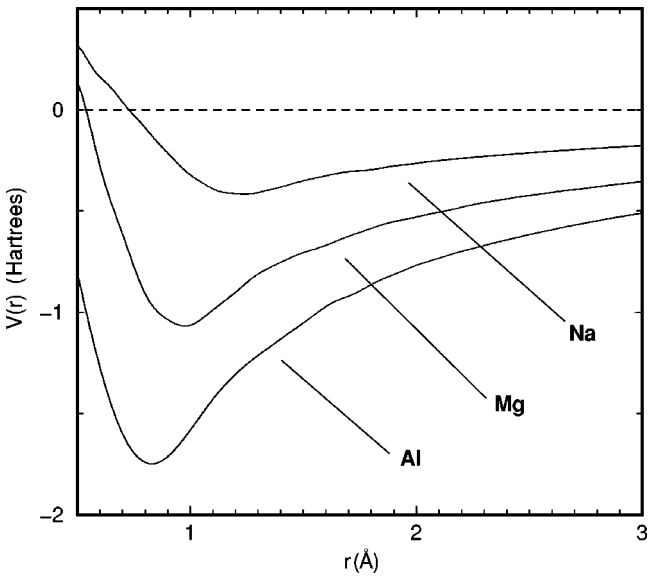

FIG. 1. Local pseudopotentials in r space utilized in this work.

tal situation in Sec. II B, the term $\delta\rho_e(\mathbf{k})$ in Eq. (10) does not occur in the simulations. Furthermore, since the Fourier coefficients occurring in Eq. (3) play a central role in the simulation process, the calculation of the partial AL structure factors by means of Eq. (2) is straightforward and does not increase the computational cost. Thus, we calculate a contribution to the averages [Eq. (2)] at each MD time step. All of the structure factors reach their asymptotic limits by $k = K_{cut}$ so that we may obtain the corresponding real-space distribution functions by back transformation [Eq. (1)]. To perform all Fourier transformations involved in this work, we have used a grid size of $dk = 0.02$ a.u. and 16 384 points. The functions in $\mathbf{k}$ space were averaged over wave vectors of the same magnitude and fitted using splines in order to interpolate onto the grid. From the maximum value available from the simulation up to the cutoff of 16 384 points, all structure factors were set equal to their long k limits. We found that direct calculation and back Fourier transformation from partial structure factors lead to the same results for the pair distribution functions.

III. SIMULATIONS AND ION-ION STRUCTURE

A. Pseudopotentials and simulation details

Three local *ab initio* pseudopotentials[20] were produced for the metals considered in this work. The electron configurations used in the initial all-electron calculations of the nonlocal *ab initio* pseudopotential were s^1p^0 for Na and s^2p^0 for Mg. For Al, a hybrid scheme was employed, in which the $l = 0$ and $l = 1$ pseudopotential components derived from an $s^2p^1d^0$ atomic configuration were combined with the $l = 2$ component of an $s^2p^0d^1$ configuration. KS solid-phase calculations (bcc lattice for Na, fcc for Mg and Al) were carried out using the CASTEP program.[13] Finally, the OF functional that describes the correct linear and quadratic response of the electron gas[19] was included in the OF computation. The real-space pseudopotentials so generated, and subsequently used in the dynamics, are shown in Fig. 1.

Details of the OF-AIMD simulations performed can be found in Table I. The three metals were simulated using the aforementioned kinetic-energy functional (including quadratic response) and the time-step to integrate the equations of motion was set equal to 20 a.u. (0.4836 fs) in all cases. The parameters employed were found to be appropriate to achieve an efficient minimization of the electronic energy for quenched configurations and a good conservation of the total energy in the dynamics. Simulations were initiated from solidlike configurations that were heated, cooled down, and equilibrated in approx. 10 000 steps (5 ps). Once equilibration was finished, long production runs of 20 000 steps (around 10 ps) were executed in order to determine the partial structure factors via Eq. (2). The required thermal average was computed by sampling over the same number of configurations. Both ion and electron movements were thermostated using Nosé-Hoover chains.[24] The production runs of 20 000 steps lasted 49–57, 52, and 200 h on a Silicon Graphics R10000 for Na, Mg, and Al, respectively.

Na and Al were simulated at two different set of conditions. In runs 1, 3, and 5 the density was fixed to the experimental value of the metal at the simulation temperature that was close to the melting point. On the contrary, runs 2 and 6 were carried out at a density slightly lower (by 5% in Na, and 6% in Al). We performed a single long run for Mg setting the density to its melting point value but with the temperature at 1000 K, since these are the parameters utilized by Wijs *et al.*[15]

B. Ion-ion structure factors and the thermodynamic state

Figure 2 shows results for $S_{II}(k)$ calculated directly from the averages over the Fourier components of the ion density at each of the k points used in the simulation. No smoothing or further averaging over these values has been performed. The figure also shows experimental results for the structure factors.[25] Apart from a slight mismatch at the principal peak of the structure factor, which we will discuss below, the agreement between the experimental and AIMD results at the experimental densities (i.e., run 1 for Na, 5 for Al, and 4 for

TABLE I. Simulation parameters for Na, Mg, and Al.

	Run	N	K_{cut}/Å	T/K	ρ/Å^{-3}	$\langle P\rangle$/a.u.
Na	1	128	7.9	400	0.0241	-2.44×10^{-5}
Na	2	128	7.8	400	0.0230	-2.52×10^{-5}
Na	3	88	6.5	400	0.0241	-2.18×10^{-5}
Mg	4	108	9.7	1000	0.0371	-2.42×10^{-5}
Al	5	115	14.6	933	0.0533	9.66×10^{-5}
Al	6	115	14.2	1000	0.0497	7.48×10^{-7}

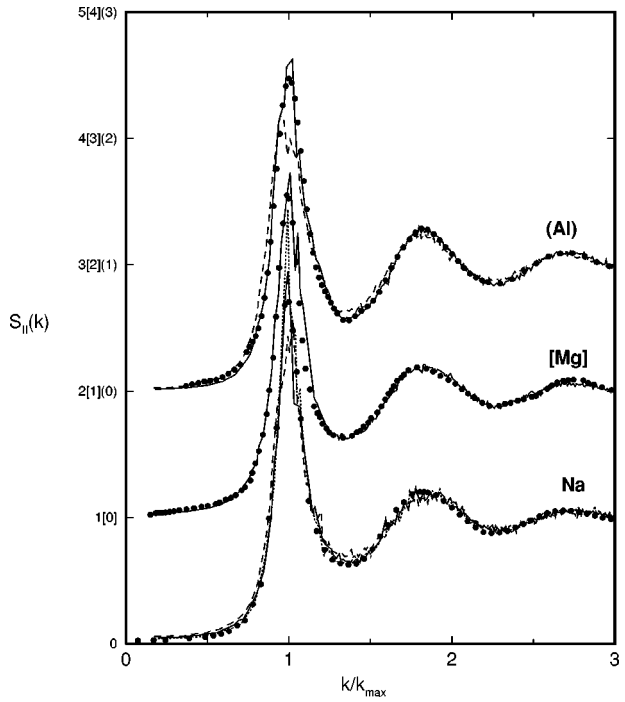

FIG. 2. Ion-ion partial structure factors of Na, Mg, and Al obtained from OF-AIMD (solid lines: runs 3, 4, and 5; dashed lines: runs 2 and 6; dotted line: run 1) and x-ray-diffraction experiments (Ref. 25) at 383, 953, and 943 K, respectively (solid circles). The structure factors are plotted against the reduced wave vector k/k_{max}, where k_{max} is the position of the first peak in $S_{II}(K)$ for that system.

Mg) is extremely good. Excellent agreement is also found in the corresponding real-space comparison shown in Fig. 3 (despite the slight mismatch). That the agreement is not accidental is confirmed by comparing the experimental structure factors (or radial distribution functions) at the melting density for Na and Al with simulation results at densities

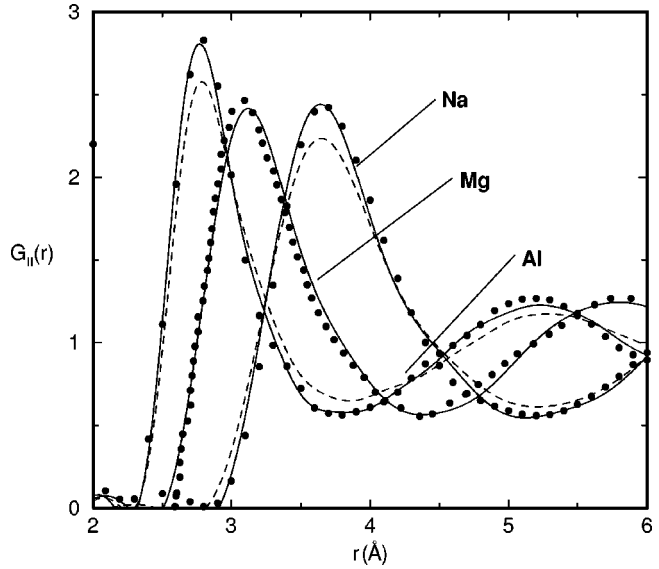

FIG. 3. Ion-ion pair distribution functions of Na, Mg, and Al. Solid lines correspond to runs 1, 4, and 5, respectively, whereas the dashed lines represent the results from runs 2 and 6 for Na and Al. The black circles are the experimental data (Ref. 25).

lower by 5% (runs 2 and 5, respectively). The small change in the mean interionic separation results in very noticeable discrepancies between the experimental and simulation curves. Table I shows the pressures of the MD runs at the experimental densities. Since these correspond to orthobaric conditions, these pressures should ideally be zero. The pressures obtained are small (by the usual standard of computer simulations) and are very similar to the pressures that need to be applied in simulations of the zero-temperature crystal to bring the calculated lattice constant into agreement with the experimental one. The lattice constants calculated with the OF-AIMD method are very similar to those obtained in the KS-AIMD calculations used in pseudopotential construction.[20] Overall, we conclude that the OF-AIMD scheme is giving an excellent description of the local ionic structure and effective interionic interactions in these metals.

As already reported in Ref. 18, we find the height of the mean peak in the partial structure factors is extremely sensitive to small variations in the simulation conditions when the calculation is performed in the proximity of the melting point. This behavior is clearly seen in the Na simulation at the experimental melting density (run 1), where the first peak reaches a value above the Verlet-Hansen[26] limit of 2.8. At a slightly lower density (run 2), this sort of effect in the structure factors does not occur. A similar behavior was observed in Al, where the run at the experimental melting density and temperature (run 5) led to excellent results for the ion-ion structure factor, save in the region of the main peak. When the density is decreased (run 6) the first peak is substantially reduced in height. We believe that the additional order, responsible for this enhancement, is induced by the periodic boundary conditions and exacerbated in these materials by the fact that the liquid and solid densities at melting are quite close (less than 2% for Na). The periodic boundary conditions may be thought to induce an additional external potential,[27] which tends to induce crystalline order and whose effect is particularly pronounced at the peak of the structure factor, where the fluid's susceptibility to periodic external potentials is largest. The problem seems to be a general one (and not an aspect of AIMD), at least when the liquid and solid densities are very similar, since, in long simulations of liquid sodium with an effective pair potential,[28] a similar effect is found. As shown in the data for run 3, we can reduce the effect by working with a number of atoms that is well away from the ''magic'' numbers for which the system may form a cubic crystalline structure commensurate with the periodic boundary conditions (simulations are normally done with such a number to facilitate the startup). In run 3, 88 atoms are used at the experimental melting density. The anomalous enhancement of the first peak seems not to occur. In the calculations reported here, the effect is associated with only a very small change in the actual fluid structure, as witnessed by the excellent agreement of the radial distribution functions with experiment.

IV. ION-ELECTRON CORRELATIONS

A. Results for S_{Ie} and comparison with KS-AIMD results

Figure 4 shows the ion-electron structure factors calculated from the various OF-AIMD runs via Eq. (2). A systematic change in shape of $S_{Ie}(k)$ in the series Na-Mg-Al is

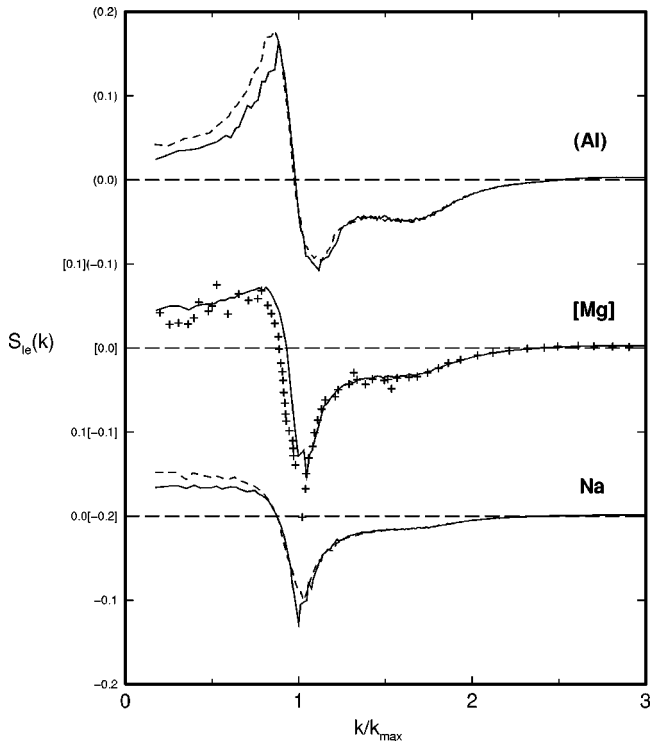

FIG. 4. Ion-electron structure factors from runs 1, 4, and 5 (solid lines) and 2 and 6 (dashed lines). The crosses denote the KS-CP results of Wijs *et al.* (Ref. 15) k_{max} is the position of the first peak in $S_{II}(K)$.

noticeable; as we shall show below, the change of shape is readily interpreted as a consequence of the increasing number of valence electrons. From the height of the main peak in the structure factor, we infer an increasing strength in the ion-electron correlation along the series. This follows naturally from the fact that the pseudopotentials generated for these systems have deeper energy wells for the ions with higher charges. The progressive enhancement in the strength of correlation may also be seen in real space. Figure 5 shows the ion-electron radial distribution functions in the various

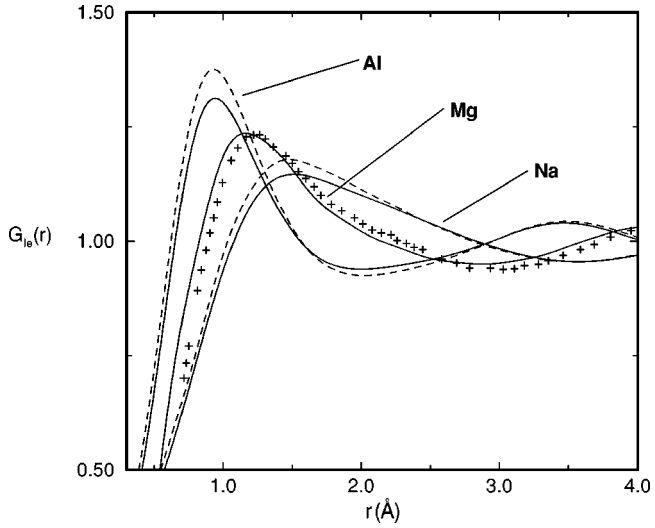

FIG. 5. Ion-electron pair distribution functions from runs 1, 4, and 5 (solid lines) and 2 and 6 (dashed lines) in Table I. The crosses represent the KS-CP results of Wijs *et al.* (Ref. 15).

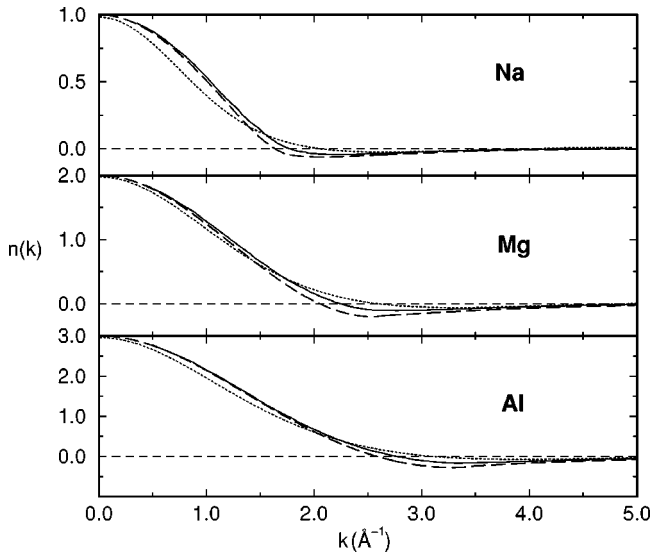

FIG. 6. Screening densities $n(k)$ obtained from runs 1, 4, and 5 in Table I (solid lines). The dashed lines represent the prediction of the linear-response theory including exchange-correlation effects (see text) and the dotted lines correspond to the valence electron density of an isolated atom.

runs. The reduction in the effective atomic radii with increasing valence charge is clearly evident from this figure. These figures also show an increase in the strength of the ion-electron correlation as the fluid density is lowered. In viewing this figure it should be recalled that the true valence electron density has been replaced by a *pseudodensity* that only matches the true density outside the core region. However, in calculations on the isolated atom, with the pseudopotentials in use here, the pseudodensity agrees closely with the true density down to distances of order 0.7 Å, so that, within the range of r values spanned, the figure should be giving a reliable representation of the true ion-electron radial distribution function.

Figures 4 and 5 also show the data for Mg obtained by de Wijs *et al.*[15] using the KS-AIMD method at the same density and temperature. Excellent agreement between the two sets of data is evident. This is an important result in the validation of the OF-AIMD procedure. The better statistical precision of our results is apparent at low k.

B. The screening density and the predictions of linear-response-theory

By using Eq. (12) we can extract results for the effective screening density n of the valence electrons around the ion cores. Results for this quantity are shown in Fig. 6. The screening density, in reciprocal space, may be regarded as the effective form factor for the valence electrons, as seen in Eq. (14). As such, it may be usefully contrasted with the valence form factor for the free atom, which may be calculated from the Fourier transform of the densities of the valence orbitals. These densities are obtained from the all-electron KS calculations used in the pseudopotential generation procedure. This is shown by the dotted line in the figure. Figure 7 shows the screening density in real space compared with the free atom valence electron density. The comparison shows that the limitations imposed by the use of

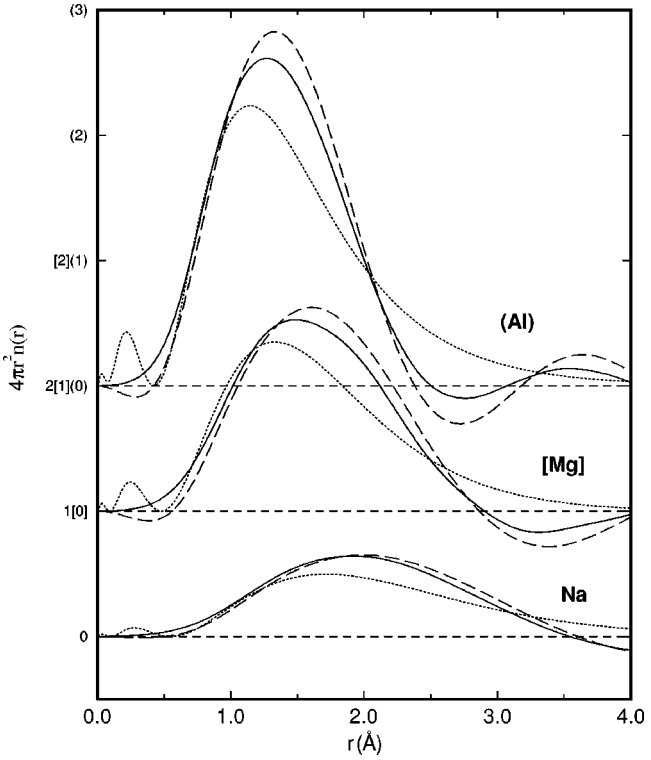

FIG. 7. Spherically integrated screening densities in real space. The lines have the same meaning as in Fig. 6.

the pseudodensity are not large. Figure 7 also indicates that when the atom is immersed in the sea of conduction electrons in the metal there is an enhancement of the valence electron density close to the nucleus (i.e., in the range of the main peak in the density) and a reduction of the density at slightly longer range: the displacement of the screening density is more marked the higher is the ionic charge. At larger distances the screening density oscillates about the average electron density of the metal; this is responsible for the oscillatory character of the effective interionic pair potentials of metals.[1] Very similar behavior has been predicted by means of the quantal hypernetted chain theory.[6,7]

The consistent *shape* of the screening density in reciprocal space (Fig. 6) for Na, Mg, and Al, enables us to interpret the evolution of the ion-electron structure factor $S_{Ie}(k)$ (Fig. 4) passing from Na to Al, i.e., with an increasing number of valence electrons.[29] As seen from Eq. (12), $S_{Ie}(k)$ is the product of $n(k)$ and $S_{II}(k)$ and the latter has a very similar shape in all the metals, the k scale being set by the position of the first peak of the structure factor k_{max} (Fig. 2). Since, $n(k)$ is positive at small k and first passes through zero at a value k_0 that steadily increases with the density of valence electrons, the shape of $S_{Ie}(k)$ can be seen to be determined by the relationship of k_{max} to k_0. For Na, k_{max} is significantly greater than k_0, and the main peak of $S_{II}(k)$ appears as a negative feature in $S_{Ie}(k)$. In Mg k_{max} is slightly smaller than k_0, and some of the main peak occurs in a region where $n(k)$ is positive, whereas for the higher k part it is negative, leading to a derivative shape. The derivative shape is still more pronounced in Al where $k_{max} \sim k_0$. As expected from linear-response theory (see below), the value of k_0 is close to twice the Fermi wave vector of the valence electrons in the metal [$k_F=(9\pi/4)^{1/3}/r_s$, where r_s is the radius of the free electron sphere]. Values for the ratio $k_0/2k_F$ were found to be 0.991(Na), 0.858(Mg), and 0.804(Al). Hence, the shape of $S_{Ie}(k)$ is primarily determined by the relationship between the mean interatomic and interelectron separations.

It is very interesting to contrast the results emerging from the OF-AIMD simulations for the ion-electron correlations with those predicted by linear-response theory. On the one hand, the LRT results (as we shall see) provide a ready interpretation of the shape of $n(k)$, and hence of the shape of $S_{Ie}(k)$. On the other hand, the construction of the orbital-free kinetic-energy functional[16,18] is heavily based on results of response theory and guarantees correct linear response (within the local-density approximation of DFT). It is of interest to see to what extent the higher-than-linear response of the electron gas influences the results for the ion-electron correlations.

Within the framework of linear-response theory, the effect of each ionic core on the valence electron charge distribution can be considered independently and calculated from the response of an uniform electron gas at the density of the conduction electrons to the presence of the ion-electron potential:[1,30]

$$n_{LRT}(\mathbf{k}) = \chi^0(\mathbf{k}) V_{Ie}(\mathbf{k}), \tag{20}$$

where $\chi^0(\mathbf{k})$ is the *external* response function or susceptibility of the (interacting) electron gas and $V_{Ie}(\mathbf{k})$ is the ion-electron potential. $\chi^0(\mathbf{k})$ is normally expressed in terms of the random phase approximation for the screened response function χ_L (the Lindhard function[31])

$$\chi^0(\mathbf{k}) = \frac{\chi_L(\mathbf{k})}{1+(4\pi/k^2)\chi_L(\mathbf{k})[G(k)-1]}, \tag{21}$$

where $G(k)$ is a ''local-field factor,'' which accounts for the exchange-correlation effects.[1] Wax, Jakse, and Bretonnet[11] calculated the ion-electron structure factor for the alkali elements using this formalism, the Ichimaru-Utsumi[32] local-field factor and the Shaw pseudopotentials[33] and obtained results in good accord with ours for Na.

We have calculated the LRT predictions for the screening density in Na, Mg, and Al by using the Ichimaru-Utsumi local-field factor in $\chi^0(\mathbf{k})$.[32] We have previously shown that the effective linear-response function within our orbital-free calculations is very similar to this theoretical result for $\chi^0(\mathbf{k})$. We have used the same local OF pseudopotential, obtained from the *ab initio* KS nonlocal potential, as used in the OF calculations. It should be noted that the pseudopotentials normally used in LRT-based calculations of the effective interionic interactions in metals are substantially softer in the core region than such *ab initio*-based potentials; this is true of the Shaw potentials used by Wax, Jakse, and Bretonnet,[11] for example. As stressed by Hafner,[1] they are potentials appropriate to the application of LRT and would not (in general) reproduce the actual valence orbitals of an atom in the way that KS pseudopotentials do. The results in Figs. 6 and 7 show that the *ab initio*-based potentials are too strong for their effect to be described by LRT, even, as noted previously,[16] in the case of Na. [The discrepancy in the reciprocal space function would be more noticeable were we to plot $k^2 n(k)$]. In Fig. 7 we see that the screening density becomes negative inside the ionic cores, and that the oscil-

lations at longer range are too large. The discrepancy between the OF results and the LRT ones becomes more pronounced along the series Na-Mg-Al. Conversely, these results show that the *ab initio* KS-based pseudopotentials induce significant higher-order responses in the electron density and, recalling the excellent correspondence between the OF and KS results for Mg, that the OF method is capturing these higher-order effects successfully. This is an important conclusion since *ab initio* KS-based pseudopotentials should be *transferable* to different phases of the metal and its alloys.

Nevertheless, the LRT calculated screening densities show qualitatively many of the features present in the full OF calculations. In particular, the shape of $n(k)$ and the position of the first zero crossing k_0, invoked in the discussion of the behavior of $S_{Ie}(k)$ above, are very similar. This therefore enables us to trace the shape of $S_{Ie}(k)$ back to the response function. The k dependence of $\chi^0(\mathbf{k})$, the scale of which is set by k_F, is what determines the characteristic shape of the screening density seen in Fig. 6.

C. Comparison with experimental results for the ion-electron correlation

Takeda *et al.*[10] have obtained experimental results for the ion-electron correlations in Na, Mg, and Al by combining the x-ray- and neutron-scattering data. They present results for the ion-electron structure factor that may be directly compared with ours appearing in Fig. 4. We find that the experimental results differ markedly from ours. If we focus on Na, the experimental results have a similar shape to ours; the main dip appears at ~ 1.9 Å^{-1}, in good agreement, but it is considerably deeper than we find ~ 0.25 vs ~ 0.15. For Mg, even the shape of the experimental function differs substantially from ours (which, as noted above, is fully consistent with the KS-AIMD results of de Wijs[15]). For Al there are again substantial discrepancies with the shape of the function resembling that obtained for Na, with no positive first peak and a dip very much greater than the amplitude of our function. The experimental results therefore do not show the systematic trend from Na-Mg-Al which, as explained above, is qualitatively described by response theory. Overall, the experiments suggest a stronger ion-electron correlation than is predicted from theory and simulation.

In order to cast some light on the origin of these disagreements, we have calculated an estimate of what the difference between the x-ray- and neutron-diffraction structure factors should be. In order to do this, we make use of Eq. (15) for the x-ray structure factor. We obtain the form factors $f_I(k)$ and $f_A(k)$ required in Eq. (15) by means of all-electron KS calculations in the isolated ion/atom and subsequent Fourier transform of the total ionic/atomic charge density. Our results for the difference between the coherent x-ray and neutron structure factors are plotted in the lower part of Fig. 8. In the upper panels of this figure we show the experimental results[10] for the difference between the coherent x-ray and neutron-scattering structure factors.

The most striking features of the curves are in the vicinity of the principal peak of the ion-ion structure factor. The amplitudes of the experimental results in this régime are an order of magnitude above their theoretical counterparts. In fact, the functions extracted from our calculations are almost

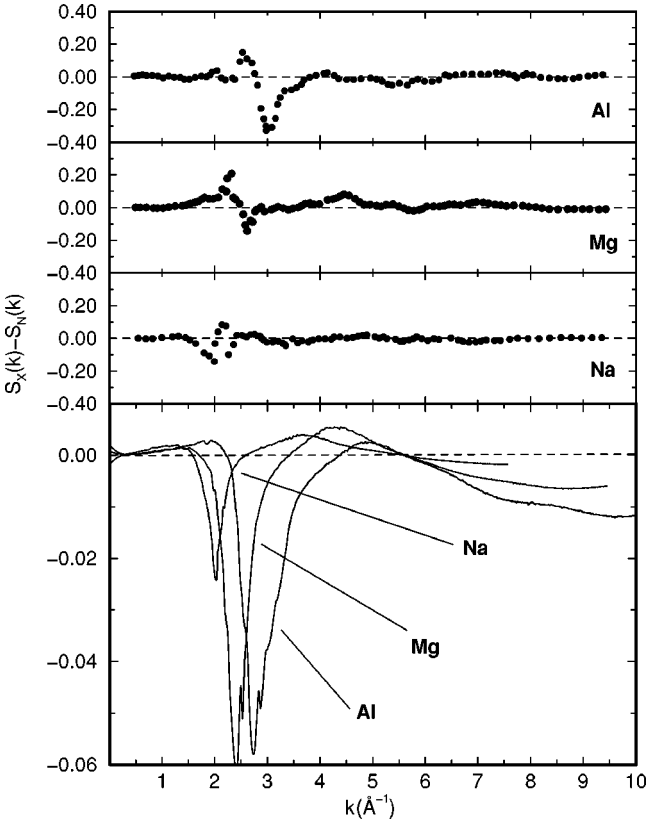

FIG. 8. Difference between x-ray- (S_X) and neutron- (S_N) diffraction structure factors from scattering measurements (Ref. 10) (upper panels) and as derived from runs 1, 4, and 5 in Table I (lower panel).

within the reported experimental uncertainty [~ 0.02 (Ref. 10)] for the structure factors $S_X(k)$ and $S_N(k)$. We further note the progressive evolution of the shape of this feature in the theoretical results, as the number of valence electrons is increased, in contrast to the unsystematic evolution of the experimental quantities. Another notable difference between two sets of data is that our results for the difference die away to zero very slowly with increasing k, so slowly, in fact, that the ultimate decay has not been approached within the window shown in the figure. The reason for this slow decay lies entirely in the ratio between the ionic and atomic form factors at these values of k. Both form factors approach zero asymptotically, but we have not reached this asymptotic region at $k=10$ Å^{-1}. We should stress that this finding is not affected by the pseudopotential approximation, since the calculated form factors are obtained from all-electron calculations. Our results for these form factors agree well with the normally tabulated[34] results, but are not affected by having been fit to standard functional forms.

According to our *ab initio* calculations, the difference between x-ray and neutron structure factors should be much smaller than so far observed in the diffraction measurements. This conclusion is in accord with the findings of a number of previous works for individual examples from the Na, Mg, Al set.[7,11] The finding that the difference is small is not surprising when it is realized that the valence charge density does predominantly behave as a screening density, which simply follows the ions as they move around in the fluid, and that this screening density is quite similar to the free atom va-

lence density. The effective ionic form factor in the liquid is therefore similar to that of the free atom. This viewpoint has previously been expressed by Chihara and Kambayashi.[7] Hence, the only mechanism that could lead to a significant difference between x-ray and neutron experiments would come from the part of the electron-electron scattering that is uncorrelated with the nuclear positions. However, as stressed by Chihara,[4] this uniform background of electrons generates *incoherent* scattering and, therefore, must not be included in the experimental $S_X(k)$.

V. CONCLUSIONS

We have carried out a comprehensive study by means of orbital-free-AIMD simulation of the ionic and electronic structure of three typical liquid metals. The calculated ionic structure factors and radial distribution functions are in excellent agreement with experiment. Comparison of the OF-AIMD results with Kohn-Sham AIMD results for Mg have shown that the OF technique is capable of reproducing the Kohn-Sham results for the ionic and electronic structure of this system at a small fraction of the computational cost. Analysis of the screening density of the valence electrons around the ionic cores shows that, even in sodium, this is not accurately described as the *linear* response of a uniform sea of electrons when *ab initio* (Kohn-Sham) pseudopotentials are used, and that the OF-AIMD does recapture the beyond-linear effects. Nevertheless, the linear-response calculation does reproduce the main features of the screening density, in particular, the period of the Friedel oscillations. This therefore enables an interpretation of the shape of the ion-electron structure factor and of its evolution with the number of valence electrons in the series Na-Mg-Al. The ion-electron structure factor can, in principle, be extracted from a comparison of the x-ray and neutron structure factors. We have calculated the difference between the predicted x-ray and neutron structure factors and find it to be significantly smaller than has so far been found in experimental studies for these metals. It is clear that the extraction of reliable information on the ion-electron correlations in these liquids places very strong demands on the treatments of incoherent contributions to the x-ray scattering and of the different resolutions of the x-ray and neutron methods.

ACKNOWLEDGMENTS

P.A.M. is grateful to Ard Louis for a stimulating discussion about the ion-electron structure factor and we acknowledge the help of Phil Salmon in clarifying the relationship between the calculated quantities and experiment. J.A.A. thanks the Ministerio de Educación y Cultura of Spain for partial financial support. This work has been supported by EPSRC Grant No. GR/L49369 and by the UKCP consortium.

[1] J. Hafner, *From Hamiltonians to Phase Diagrams* (Springer-Verlag, Berlin, 1987).
[2] P. A. Egelstaff, N. H. March, and N. C. McGill, Can. J. Phys. **52**, 1651 (1974).
[3] P. J. Dobson, J. Phys. C **11**, L295 (1978).
[4] J. Chihara, J. Phys. F **17**, 295 (1987).
[5] K. Hoshino and M. Watabe, J. Phys. Soc. Jpn. **61**, 1663 (1992).
[6] M. Ishitobi and J. Chihara, J. Phys.: Condens. Matter **4**, 3679 (1992).
[7] J. Chihara and S. Kambayashi, J. Phys.: Condens. Matter **6**, 10 221 (1994).
[8] S. Takeda, S. Harada, S. Tamaki, and Y. Waseda, J. Phys. Soc. Jpn. **58**, 3999 (1989).
[9] S. Takeda, M. Inui, S. Tamaki, K. Maruyama, and Y. Waseda, J. Phys. Soc. Jpn. **63**, 1794 (1994).
[10] S. Takeda, Y. Kawakita, M. Inui, K. Maruyama, S. Tamaki, and Y. Waseda, J. Non-Cryst. Solids **205-207**, 365 (1996).
[11] J.-F. Wax, N. Jakse, and J.-L. Bretonnet, Phys. Rev. B **55**, 12 099 (1997).
[12] R. Car and M. Parrinello, Phys. Rev. Lett. **55**, 2471 (1989).
[13] M. C. Payne, M. P. Teter, D. C. Allan, T. A. Arias, and J. D. Joannopoulos, Rev. Mod. Phys. **64**, 1045 (1992).
[14] R. G. Parr and W. Yang, *Density-Functional Theory of Atoms and Molecules* (Oxford University Press, Oxford, 1989).
[15] G. A. de Wijs, G. Pastore, A. Selloni, and W. van der Lugt, Phys. Rev. Lett. **75**, 4480 (1995).
[16] M. Pearson, E. Smargiassi, and P. A. Madden, J. Phys.: Condens. Matter **5**, 3221 (1993).
[17] E. Smargiassi and P. A. Madden, Phys. Rev. B **49**, 5220 (1994).
[18] M. Foley, E. Smargiassi, and P. A. Madden, J. Phys.: Condens. Matter **6**, 5231 (1994).
[19] M. Foley and P. A. Madden, Phys. Rev. B **53**, 10 589 (1996).
[20] S. Watson, B. J. Jesson, E. A. Carter, and P. A. Madden, Europhys. Lett. **41**, 37 (1998).
[21] J. P. Hansen and I. R. McDonald, *Theory of Simple Liquids* (Academic, New York, 1986).
[22] G. B. Bachelet, D. R. Hamann, and M. Schlüter, Phys. Rev. B **26**, 4199 (1982).
[23] N. Troullier and J. L. Martins, Phys. Rev. B **43**, 1993 (1991).
[24] G. J. Martyna, M. J. Klein, and M. Tuckerman, J. Chem. Phys. **97**, 2635 (1992).
[25] IAMP database of [SCM-LIQ], http://www.iamp.tohoku.ac.jp
[26] L. Verlet, Phys. Rev. **165**, 201 (1968).
[27] A. R. Denton and P. A. Egelstaff, Z. Phys. B **103**, 343 (1997).
[28] F. Shimojo, K. Hoshino, and M. Watabe, J. Phys. Soc. Jpn. **63**, 141 (1994).
[29] Ard Louis (private communication).
[30] N. W. Ashcroft, *The Liquid State of Matter: Fluids, Simple and Complex*, edited by E. W. Montroll and J. L. Lebowitz (North-Holland, Amsterdam, 1982).
[31] N. W. Ashcroft and N. D. Mermin, *Solid State Physics* (Holt-Saunders, New York, 1976).
[32] S. Ichimaru, Rev. Mod. Phys. **54**, 1017 (1982).
[33] R. W. Shaw, Phys. Rev. **174**, 769 (1968).
[34] *International Tables for X-ray Crystallography* (The Kynoch Press, Birmingham, England, 1974), p. 99.